Hindawi
Shock and Vibration
Volume 2018, Article ID 7569432, 12 pages
https://doi.org/10.1155/2018/7569432

Research Article

Characterization of Flow Separation around Inline Cylinders within Oscillatory Flow

Yiding Zhao[1] **and Yao Shi**[2]

[1]*School of Civil Engineering, Central South University, Changsha 410075, China*
[2]*Cccc WuHan Harbour Engineering Design and Research Co.Ltd, Wuhan 430000, China*

Correspondence should be addressed to Yiding Zhao; zhaoyiding89@126.com

Received 21 June 2018; Accepted 9 September 2018; Published 15 October 2018

Academic Editor: Francesco Franco

This paper has examined the effects of Reynolds number (Re), Keulegan–Carpenter number (KC), and gap ratio on flow separation around a cylinder array by PIV method in experiment. The vortex shedding in such situation occurs each half period of the oscillatory motion from the observation. No matter how many cylinders, KC is the key dominant parameter under low Re that has a great impact on the flow regime and flow motion in oscillatory flows. There is an influence area of vortex shedding around the cylinder. When two inline cylinders are in the flow, smaller gap ratio may extend the influence area of the vortex shedding. For $s/d = 2$, the vortex shedding that happens in each cylinder has a simultaneity and independence. For $s/d = 1.5$, the reduced gap ratio leads the upstream shed vortex to interact with downstream cylinder and makes the influence area of vortex shedding around downstream cylinder extends further. For $s/d = 1$, the interference in the central area is significantly obvious and the vortex shedding is suppressed and even follows the cross gap flow.

1. Introduction

Flow separation around a single cylinder is well understood [1] that hydrodynamics around a single cylinder in both steady current and oscillatory flows from two aspects which are flow regimes and forces. For a cylinder in steady current, the flow regimes are dependent on the cylinder Reynolds number (Re). With increasing Re, vortices would be produced in the wake region of the cylinder.

Vortex shedding occurs at either side at a certain frequency in the wake region when Re is above 40. The turbulent boundary layer separation occurs at one side of cylinder with laminar at the other side in $3*10^5 < \mathrm{Re} < 3.5*10^5$ [2], which can cause significant nonzero mean lift on the cylinder. The two-dimensional vortex shedding occurs in the range of $40 < \mathrm{Re} < 200$ and the model of vortex shedding is laminar [3]. It will remain unchanged in the span direction. The critical Reynolds number for the onset of vortex shedding is determined to be 47 [4]. On the other hand, the same conclusion can be drawn that the vortex shedding turns into three-dimensional, and vortices are shed in cells in the spanwise direction in the range of $200 < \mathrm{Re} < 300$ [5]. Specifically, the onset of three-dimensionality is already observed at $\mathrm{Re} = 160$ as confirmed numerically and experimentally [6]. The ratio for the friction drag to the total drag force is less than 4% with $\mathrm{Re} > 10^4$ so that the friction drag is unimportant to be ignored in the total mean drag [7]. The aperiodic shedding regime may occur at certain KC and Re within switching between different modes in numerical ways [8]. The Hybrid Lagrangian/Eulerian discrete vortex method was used to simulate oscillatory flow around a cylinder [9], which has a good agreement with the experimental data.

The interaction of vortex systems between a pair of side-by-side square cylinders in numerical, which demonstrated that different gap ratio of cylinders, plays an important role in the vortex shedding of side-by-side cylinders for a certain Keulegan–Carpenter number (KC) value [10]. The effects of different KC values have been studied by finite-element simulation, which is based on the oscillatory flows around four cylinders in square arrangement of 2 times gap ratio [11]. A direct-forcing immersed boundary method [12] is developed to simulate the hydrodynamic loading on circular cylinder array in oscillatory flow, from which the results are

consistent with a previous study [11]. LBM (Lattice Boltzmann method) in numerical and PIV (particle image velocimetry) is used [13] in experiment to investigate the flow around six inline square cylinders in steady current, which pointed out the gap ratio is important for flow regime [14]. All the research has indicated the importance of gap ratio on the flow regime formation around a cylinder array. However, no one has observed flow separation around a cylinder array in the experiment. From the previous literatures, four leading factors should be vital to the flow separation around a cylinder array in oscillatory flows, which are Re, KC, gap ratio, and the number of cylinders Therefore, an experiment was conducted to observe flow separation around a cylinder array, herein limited as two aligned cylinders, in oscillatory flows, and the analysis is presented in this paper.

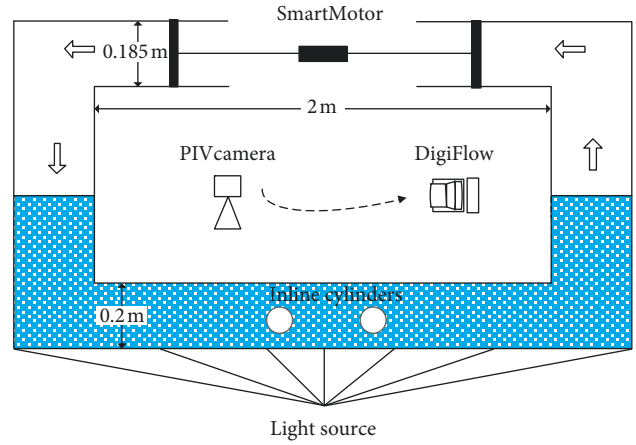

Figure 1: Sketch of experiment device.

2. Methodology

2.1. Experimental Setup. The experiment is conducted in a U-tube with a computer-controlled machine called SmartMotor [15] which can provide the oscillatory flows, as shown in Figure 1. Cylinders are set up inline in the center of bottom of the U-tube. The tracer particles need to be added into the flow before the experiment, which can visualize fluid motions under a light source (below the U-tube). During the experiment process, a digital camera is set in front of the U-tube to capture the fluid motions, and then data are output to the computer in Digiflow [16]. The fluid can have different density by dissolving salt into the tap water, and the density can be adjusted for particles to make the fluid fully filled with particles so that the best observation performance of fluid motion can be achieved.

The oscillation was often formed from the oscillation of the cylinder [1, 17, 18], which has three significant shortcomings: (1) the cylinder oscillation can lead to vibration, which may have an effect on the flow stability and contribute deviation for the experiment results; (2) the movement of the cylinder means that it cannot cling to the wall, so the end effect of the cylinder cannot be neglected; (3) the cylinder oscillation is more limited to the device than the motor motion used here which causes some inconvenience for oscillation simulation. Hence, the oscillatory flow is realized through the motor motion in the airtight U-tube in this experiment.

Due to vortices formed in the wake region, the flow can be greatly complex and unstable. Particle image velocimetry (PIV) is such a method which can capture instantaneous fluid velocity with tracer particles in the whole flow fields. PIV [19] has evolved to be a dominant and standard method for velocimetry in experimental fluid mechanics [20–23], especially in researching turbulent and complex flows. The digital camera can capture the tracer particle motion under a light source with flow to reconstruct the fluid motion by interrogation in computer so that the flow velocity can be obtained.

2.2. Generation of Oscillatory Flow. SmartMotor can simulate various oscillate movements easily in many applications by setting the target position, velocity, and acceleration. The oscillatory flow will take a cosinusoid curve for simplicity in this project,

$$y = A\cos\left[\left(\frac{2\pi}{\mathrm{T}}\right)\cdot t\right], \tag{1}$$

where A is the amplitude, T is the period, and t is the time. However, two key parameters of the oscillatory flow can have a great impact on the flow separation around cylinders, Re and KC, as follows:

$$\mathrm{Re} = \frac{DU_{\mathrm{m}}}{\nu},$$
$$\mathrm{KC} = \frac{U_{\mathrm{m}}T}{D}, \tag{2}$$

where, Re is Reynolds number, KC is Keulegan–Carpenter number, D is the diameter of the cylinder of 50 mm, U_{m} is the maximum velocity, ν is the kinematic viscosity, and T is the period of the oscillatory flow. In the cosinusoid motion, longer T and smaller A make the oscillatory motion gentler. Therefore, the value of Re and KC can be controlled through adjusting frequency and amplitude of motor motion. Meanwhile, the control variate method is applied to figure out how Re and KC affect flow separation, respectively. U_{m} can be obtained from $\mathrm{U_m} \sim \mathrm{y'} = 2\pi(\mathrm{A/T})$, so Re can be obtained from Re ~ A/T and KC can be obtained from KC~A. As certain amplitude A is decided, KC is definitely the same for oscillatory flow with different periods T, and then the effect of Re can be obtained. On the other hand, for the same A/T sample group, the effect of KC can be observed by comparison of different groups.

Considering rationality of Re and KC values and the limitation of devices, values of A are set as 0.01, 0.02, 0.05, and 0.1 m and T are set as 3, 6, 9, and 12 s. As a result, the data sets are formed as shown in Tables 1 and 2.

However, when SmartMotor performs the designed motions, there will be deviations between the proposed motions and simulation motions. There is a phase difference between the designed cosine curves and simulation curves with the time going. Additionally, the phase difference gets more obvious with a longer period, which indicates that the

Table 1: Data sets for analysis of effect of Re.

Effect of Re					KC
Set 1 ($A = 0.01$ m)					
T (s)	3	6	9	12	
Re	703.0	351.5	234.3	175.8	0.8
Re(actual)	759.3	391.2	253.1	189.8	
Set 2 ($A = 0.02$ m)					
T (s)	3	6	9	12	
Re	1406.0	703.0	468.7	351.5	1.7
Re(actual)	1518.5	782.5	506.2	379.6	
Set 3 ($A = 0.05$ m)					
T (s)	3	6	9	12	
Re	3515.1	1757.5	1171.7	878.8	4.2
Re(actual)	3796.3	1956.1	1265.4	949.1	
Set 4 ($A = 0.1$ m)					
T (s)	3	6	9	12	
Re	7030.1	3515.1	2343.4	1757.5	8.4
Re(actual)	7592.5	3912.3	2530.8	1898.1	

Table 2: Data sets for analysis of effect of KC.

	Effect of KC		Re	KC
Data set	A (m)	T (s)		
1	0.05	6	1757.5	4.2
	0.1	12		8.4
2	0.01	3	703	0.8
	0.02	6		1.7
3	0.05	3	3515.1	4.2
	0.1	6		8.4

simulation frequency may be a little larger than the designed cosine movement. However, the amplitude is exactly the same for both curves. Hence, the Fourier transform is used to figure out the components of simulation motions for different frequencies. FFT (fast Fourier transform) is applied in MATLAB, which is a faster version of the discrete Fourier transform (DFT). The DFT takes a discrete signal in the time domain and transforms that signal into its discrete frequency domain representation. The result from FFT for $y = 10\cos(2\pi t/6)$ with 20-period samples are demonstrated in Figure 2(a), and the other results are not presented here. When the period is 3 s, the designed frequency f_0 is $1/\mathrm{T} = 0.33\ \mathrm{s}^{-1}$ and the dominant component of the frequency in simulated motions f_s is 0.36 s ($f_0 = 0.167\ \mathrm{s}^{-1}$ and $f_s = 0.1855\ \mathrm{s}^{-1}$ for 6 s, $f_0 = 0.11\ \mathrm{s}^{-1}$ and $f_s = 0.12\ \mathrm{s}^{-1}$ for 9 s, and $f_0 = 0.083\ \mathrm{s}^{-1}$ and $f_s = 0.090\ \mathrm{s}^{-1}$ for 12 s). The designed frequency against the simulated frequency curve is shown in Figure 2(b). As the order of magnitude of ν is significantly larger than T, the effect of frequency difference can be neglected. Meanwhile, KC is related to A. Hence, the generation of oscillatory flow is appropriate for such experiments.

3. Preliminary Experiment without Cylinders

The first stage of this experiment is to apply different oscillatory flows without cylinders to verify PIV measurement. At first, the oscillatory flow in the U-tube was considered as oscillatory Poiseuille flow. The analytical solution for oscillatory Poiseuille flow can be derived from the Navier–Stokes equation. The coordinate is set as follows: the x-axis is in the center of the channel parallel to the streamwise direction; the z-axis is perpendicular to the top and bottom walls (the spanwise direction); and the y-axis is perpendicular to the front and rear walls. In the experiment, just consider the two-dimensional flow separations so just consider the x-axis and z-axis. Therefore, the Navier–Stokes equation can be expressed as

$$\frac{\partial u}{\partial t} = -\frac{1}{\rho}\frac{\partial p}{\partial x} + \nu\frac{\partial^2 u}{\partial z^2}. \tag{3}$$

As the velocity should be just horizontal one, only $\partial u/\partial t$ is left. Meanwhile, the pressure is up to the different water pressure from the liquid level difference. As a result, $u = f(z)e^{i\omega t}$, $\partial p/\partial x = p_{\max}\ e^{i\omega t}/\mathrm{l}$, $-1/\rho\,\partial p/\partial x = \mathrm{E}e^{i\omega t}$ ($p_{\max} = \rho\mathrm{gA}$, $E = \mathrm{gA/l}$, A is the amplitude of cosine motion, and l is the length of the U-tube and it is 2 m), so use them to replace the Navier–Stokes equation to get

$$\begin{aligned} f(z)\omega i e^{i\omega t} &= -Ee^{i\omega t} + \nu\frac{f(z)^2}{\partial z^2}e^{i\omega t}, \\ \frac{f(z)^2}{\partial z^2} - f(z)\frac{\omega i}{\nu} &= \frac{E}{\nu}. \end{aligned} \tag{4}$$

Then solve this nonhomogeneous differential equation to get the velocity equation for oscillatory Poiseuille flow:

$$u(z,t) = \frac{E}{\omega}ie^{i\omega t}\left(1 - \frac{\cosh\left(z\sqrt{i\omega/\nu}\right)}{\cosh\left(a\sqrt{i\omega/\nu}\right)}\right), \tag{5}$$

where, $a = 0.01$ m, $E = gA/l$, $\omega = 2\pi/\mathrm{T}$ (T is the period of the oscillatory movement), and $\nu = 1.5\times10^{-6}\cdot\mathrm{m}^2\cdot\mathrm{s}^{-1}$.

As there is a real part and imaginary part in this equation, MATLAB is applied to demonstrate how the velocity of Poiseuille flow changes with z and t. T (period) is set as 3 s and A is 0.1 m (to compare results from experiment). t will change from 0 to 3 s, so the velocity curve at $z = 0$ in an oscillatory period is demonstrated in Figure 3 z will change from −0.01 to 0.01 m, so the velocity curve at $t = 2.3$ is demonstrated in Figure 4. Therefore, u-t curve has showed that the velocity has the same trend with the cosine oscillatory rate (same period). u-z curve presents the velocities of flows in different areas of U-tube. The flow has the same velocity and is uniform in most areas from bottom to top, but the velocity will become significantly small in the area near the bottom and top. However, the cylinder will be set up in the center of the tube, so the central area can provide the oscillatory flow with a uniform velocity. Similarly, PIV measurement also has the same results.

Oscillatory flows generated by motor with $A = 1$, 2, 5, and 10 cm and $T = 3$, 6, 9, and 12 s are simulated, and the PIV measurement is conducted for them, as shown in Figure 5. The motion with A of 10 cm and T of 3 s is too quick to capture the tracer particles so it is given up. The cross section of the motor is different from the cross section of the flow, so the continuity principle is applied to transform the motor motion to the flow motion. The cross section of the motor is a circular section with diameter D of 0.185 m, and the flow

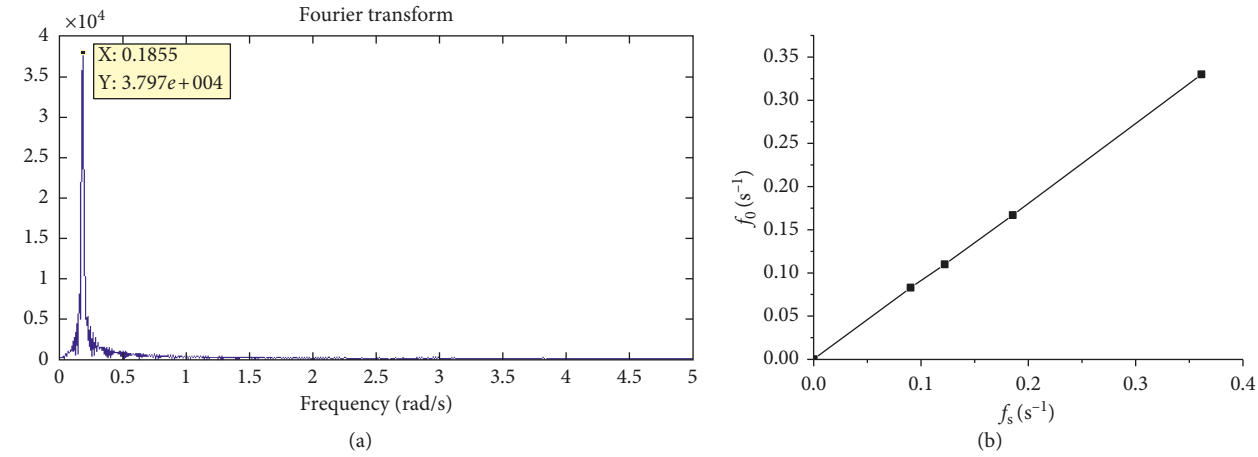

Figure 2: Discrete validation between theoretical and experimental oscillatory flow (a) FFT for $y = 10\cos(2\pi t/6)$; (b) f_0–f_s curve.

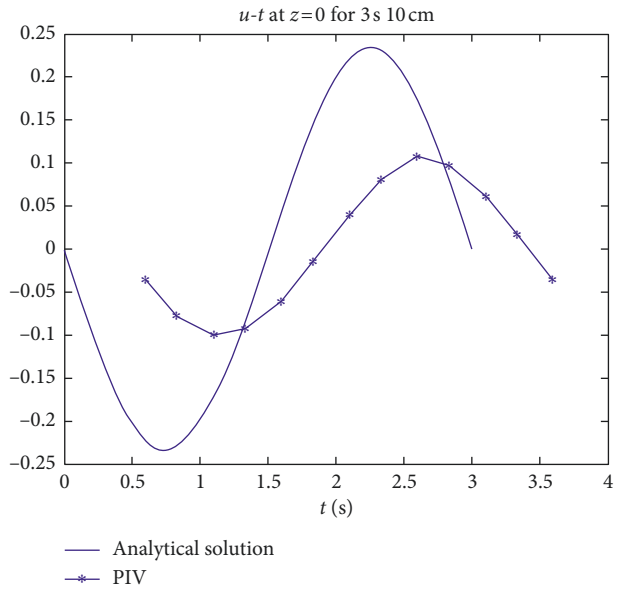

Figure 3: The PIV measurement and analytical solution for oscillatory Poiseuille flow at $z = 0$ with $T = 3$ s and $A = 0.1$ m.

section is a square section of $0.2 \times 0.2\ \mathrm{m}^2$ ($b \times b$). The continuity of the fluid is

$$A \cdot \pi \cdot \left(\frac{D}{2}\right)^2 = A_f \cdot b^2. \quad (6)$$

So, the theoretical flow amplitude A_f can be derived. Meanwhile, the uniform part of the velocity is cosine, so the theoretical maximum flow velocity also can be obtained. The whole fluid velocity field can be obtained from PIV measurement, and the average velocity from 80 mm to −80 mm is taken as the measured velocity. So the maximum measured velocity can be read from each curve, as shown in Table 3. Comparing the theoretical maximum flow velocity and the maximum measured velocity, there is a difference between them, which may be caused by friction of the motor or the interrogation of the PIV method. However, the deviation is considered to be acceptable.

4. Results of Two Inline Cylinders in Oscillatory Flow

4.1. Low KC. Two inline cylinders are set up along the center line with different distances between them. The gap ratio s/d (s is the distance between two cylinders' surfaces) is 1, 1.5, and 2. Similarly, KC is the key parameter for flow separation around two inline cylinders in low Re. When KC = 0.8 and 1.7, the same flow pattern for every single cylinder occurs as just one cylinder set in [1]. The flow around each cylinder is almost attached to the cylinder, and flow separation cannot happen with low KC. So, the interference from the upstream cylinder cannot reach to the downstream one within such spacing s/d of 1, 1.5, and 2.

4.2. KC = 4.2. When KC reaches to 4.2, a pair of vortices will form in the wake region of each cylinder with respect to streamwise. The vortex pair is still attached to each cylinder as what happens in single cylinder. The flow pattern does not change with such KC and spacing. Figure 6(a) is the typical flow pattern in such condition. However, the spacing between cylinders can have an effect on the velocity between them. According to the horizontal velocity contours for different gap ratios, the velocity in the gap is clearly decreased by 10 mm/s with the gap ratio reduced by 0.5, as shown in Figures 6(b)–6(d). Generally, low KC cannot change the flow pattern around the cylinder, but the smaller gap can decelerate the gap flow between cylinders.

4.3. KC = 8.4. In this situation, vortex shedding is supposed to occur around single cylinder, and the same is true of each one of two inline cylinders from observation, depicted in Figure 7. All experiments are conducted in Re = 3515.1 and KC = 8.4. Although the vortex shedding forms as before, the flow pattern will change in some respects with the different gap ratios. For s/d = 2, the spacing between two cylinders is far enough to form an unperturbed vortex shedding around each cylinder. Additionally, the vortex shed from left cylinder moves the same distance with that shed from right

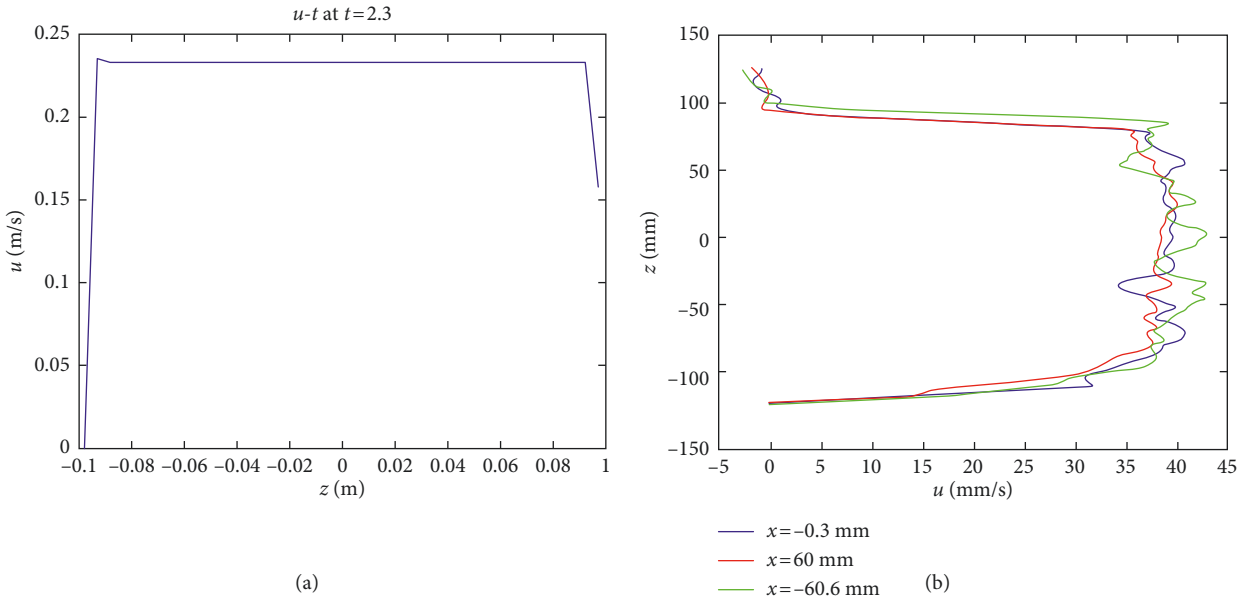

FIGURE 4: Comparison of the velocity profile for oscillatory flow. (a) Velocity profile for oscillatory Poiseuille flow at $t = 2.3$ s with $T = 3$ s and $A = 0.1$ m. (b) PIV measurement.

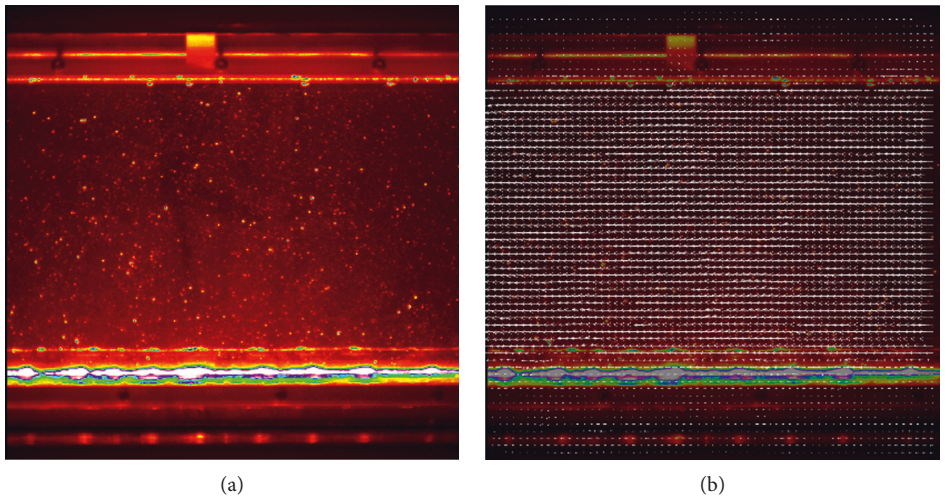

FIGURE 5: Generated oscillatory flow, (a) original record for oscillatory motion of $T = 9$ s and $A = 10$ cm, (b) cut of PIV measurement for oscillatory motion of $T = 9$ s and $A = 10$ cm.

cylinder. As a result, the second downstream cylinder can be considered to have no effect on upstream vortex shedding formation within s/d = 2. Meanwhile, the gap flow depends on the flow motion in the wake region of each cylinder. Similarly, the vortex shedding occurs at each half period of the oscillatory flow motion as single cylinder. For s/d = 1.5, the spacing is no longer long enough for each cylinder not to interfere with each other. The shed vortex from upstream cylinder reaches to the second downstream cylinder, so the vortex can interact with the downstream cylinder. It can be depicted in Figure 7(b) in which the downstream vortex shedding has propagated out of the camera range, but the downstream vortex just moves close to another cylinder. Furthermore, gap flow is affected by the downstream cylinder. For s/d = 1, such gap ratio makes a great difference on the vortex shedding. As the blockage of the second cylinder, the flow will cross the gap, which can lead to the direction change of the vortex shedding. The vortex was washed towards the top boundary by the flow crossing the gap in Figure 7(c).

However, a strange phenomenon is observed occasionally when s/d is 1.5, which is that the vortex ought to shed away from cylinder just to propagate a tiny distance, and the vortex shedding even disappears sometimes. The reason for this can be described as follows: firstly, the downstream cylinder blocks the path of vortex shedding and reflect the vortex back to upstream; secondly, the side flows put some pressure to vortex and make vortices attach to the

Table 3: Comparison of theoretical flow velocity and measured velocity.

Case	Motor amplitude A(mm)	Period T(s)	Flow amplitude a (mm)	Max flow velocity Um(mm/s)	Max measured velocity (mm/s)
1	10	3	6.72	14.1	13.1
2	20	3	13.43	28.1	26.6
3	50	3	33.58	70.3	63.5
4	10	6	6.72	7.0	6.2
5	20	6	13.43	14.1	12.3
6	50	6	33.58	35.2	30
7	10	9	6.72	4.7	4
8	20	9	13.43	9.4	8.2
9	50	9	33.58	23.4	20.6
10	100	9	67.17	46.9	42.1
11	10	12	6.72	3.5	3.2
12	20	12	13.43	7.0	6
13	50	12	33.58	17.6	15.5
14	100	12	67.17	35.2	30.9

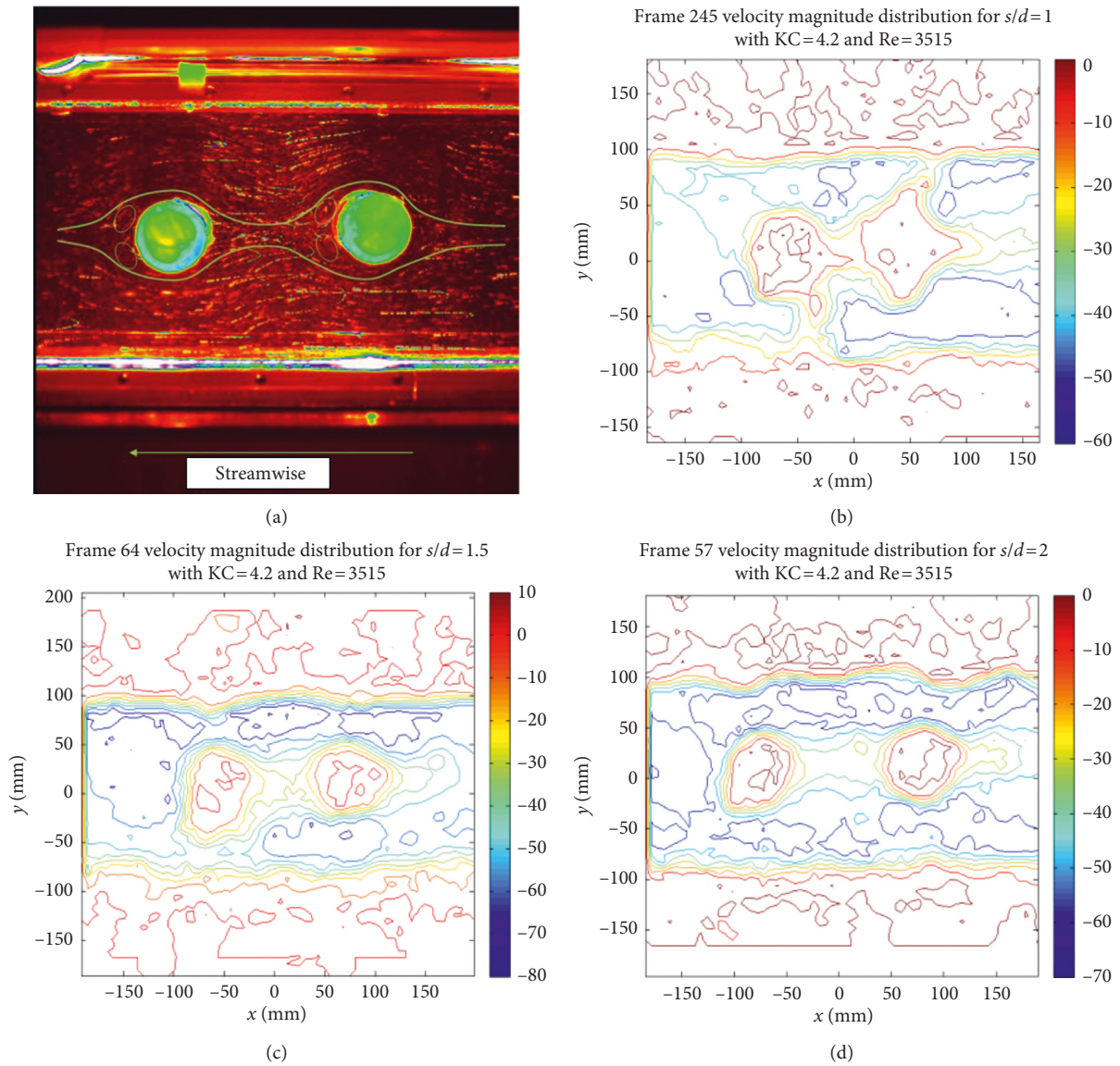

Figure 6: Outputs for KC = 4.2, (a) streaks for KC = 4.2 and Re = 3515.1 with spacing of 2, (b) horizontal velocity contours for s/d = 1, (c) horizontal velocity contours for s/d = 1.5, and (d) horizontal velocity contours for s/d = 2.

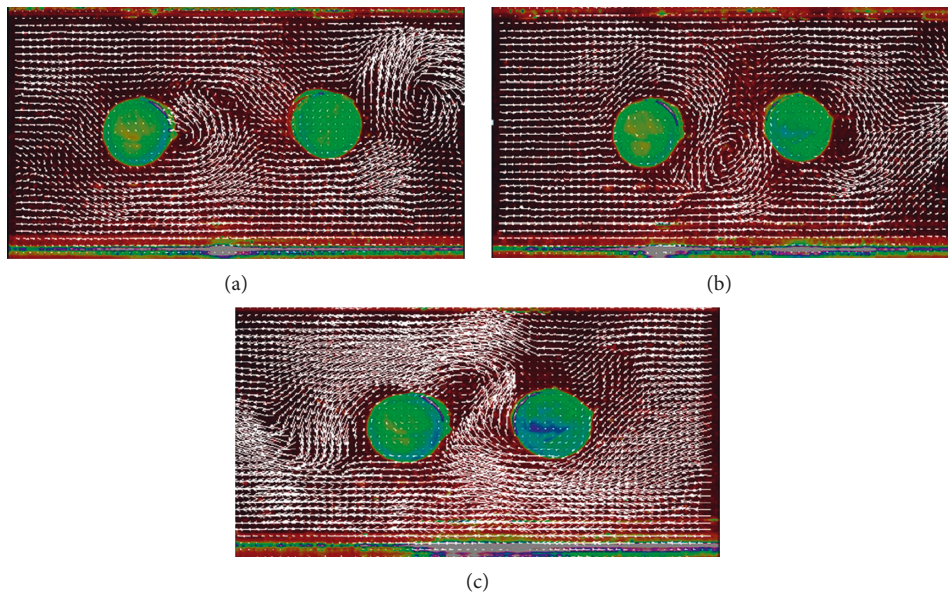

Figure 7: PIV measurement for the case with Re = 3515.1 and KC = 8.4, (a) gap ratio is 2, (b) gap ratio is 1.5, and (c) gap ratio is 1.

cylinder; and thirdly, the newly formed vortex may conflict with the old vortex formed in last half period, so the old vortex can push new one to attach the cylinder. The phenomenon will not happen within s/d = 2 because the gap is big enough while it also does not happen within s/d = 1 because the cross flow will make the vortex shed in the vertical direction.

4.4. Analysis of Velocity Profile. The coordinate is set with a null point at the midpoint in the center line between two cylinders. One second is 30 frames. The fluid velocity field is provided by PIV measurement, as well. As above, the average velocity of the edge area is regarded as the average flow velocity without cylinder or the average flow velocity not affected by the cylinder (U_0) at each frame. All the velocity here is horizontal velocity. The case in such a condition with Re = 3515.1 and KC = 8.4 is focused on to figure out the influence of gap ratio on the flow separation. The variation of the normalized velocity U/U_0 along three lateral locations is investigated. The three locations are the left and right sides of two cylinders (which are the front and wake region) and the center lateral liner between these two cylinders. In order to compare the flow separation in two wake regions of these two cylinders, the distance from the two side locations to each cylinder should be equal to distance from center to each cylinder. So, x takes ±3d for s/d = 2, x takes ±2.5d for s/d = 1.5, and x takes ±2d for s/d = 1. Figures 8–10 depict the normalized velocity and velocity contour in a half period for s/d = 2, 1.5, and 1, respectively.

For s/d = 2, these two cylinders are considered not to have an impact on the flow separation around each other, which means that variation of velocity field in the wake region of each cylinder should show a similarity, as shown in Figure 8. $x = 0$ and $x = -3$d is the wake region as the flow comes from right side, while $x = 0$ and $x = 3$d is the wake region as the flow comes from left side. These two wake regions are the same with respect to each cylinder. For both flow directions, the normalized velocity in wake region has a similar variation along y-axis. Moreover, the variation is the same with that of single cylinder. In addition, the difference of normalized velocity of two wake regions is relatively small, especially compared to that of s/d = 1 case. In other words, the same shape of these two wake-region-normalized velocity variations means that the vortex shedding happening in each cylinder has a simultaneity and independence. In the front area, the velocity at this lateral location is beyond the area of flow separation and vortex influence and keeps the same with the whole flow motion.

For s/d = 1.5, these two cylinders can affect each other, which can result in a chaotic state. However, in this situation, something strange occurred. From the first figure in Figure 9, the velocity near the cylinder in front area significantly decreased. The explanation is provided here: the distance is close enough to make the interaction of upstream vortex shedding and downstream cylinder possible. When the shed vortex is propagated to hit the downstream cylinder, it can make a contribution to cut off the vorticity source in downstream vortex shedding. So, the downstream vortex shedding is formed easily and quickly, which means that the vortex can move further. When the flow direction changes, the vortex will affect this area that converts from wake region to front region where the velocity will be decelerated. Certainly, the cylinder can block the flow, which also can cause the decelerated flow motion in front of the cylinder. Hence, the velocity decrease in front area can be observed. It can be seen in the velocity contour that a narrow band in the front area of the upstream cylinder is the slow-down area. On the other hand, the location along $x = -2.5$d is where vortex shedding is supposed to occur and vortex shedding is happening in the center area. However, the difference

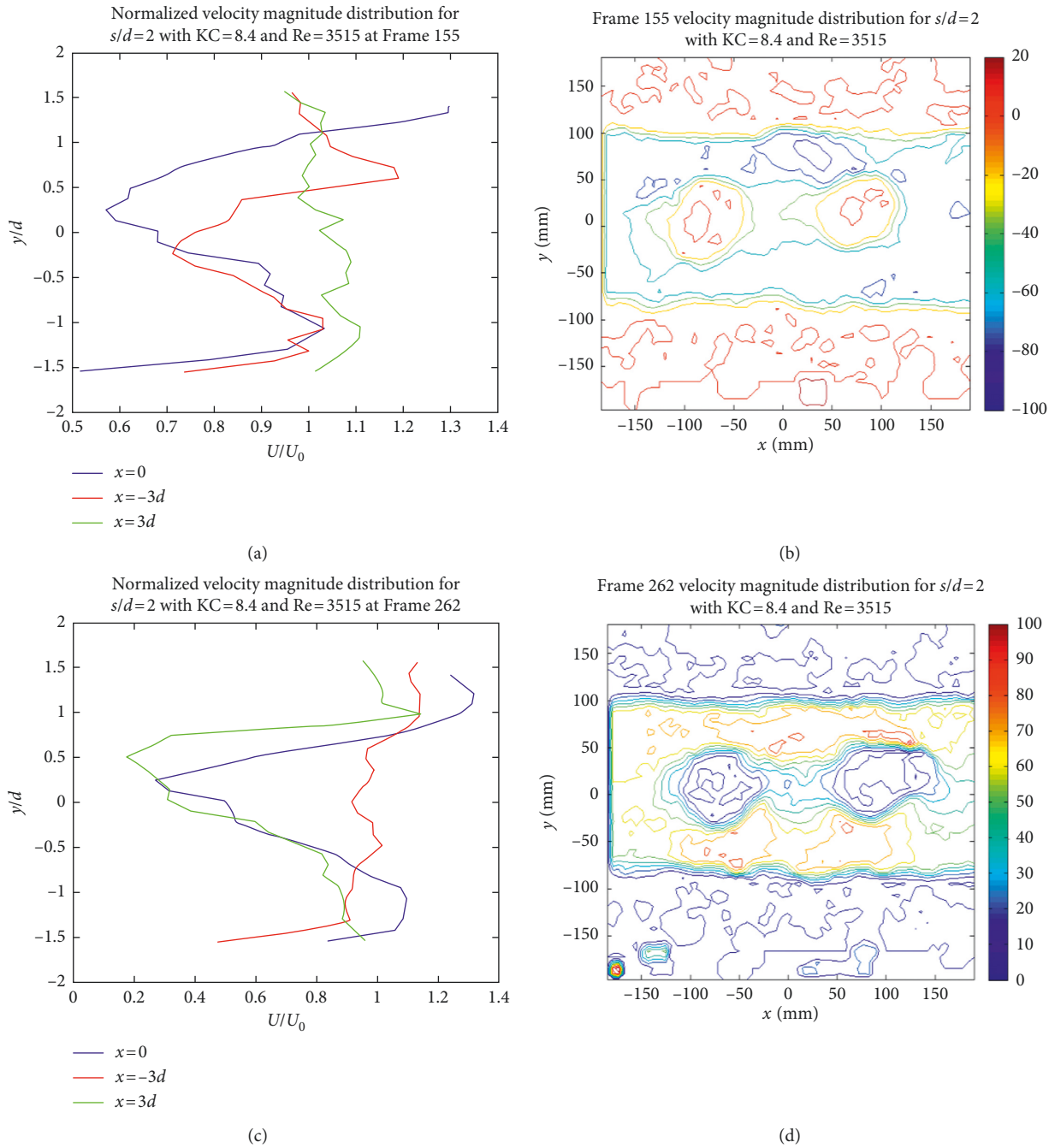

FIGURE 8: Normalized velocity and velocity contour when s/d = 2, Re = 3515.5, and KC = 8.4; (a) normalized velocity at Frame 155; (b) velocity magnitude contour at Frame 155; (c) normalized velocity at Frame 262; (d) velocity magnitude contour at Frame 262.

between them is considerably great compared with the case of s/d = 2, which means that smaller gap leads to the interference on the vortex shedding in the central area. In the next half period, the velocity in front area also behaves as before but it generally keeps pace with the whole flow motion. Meanwhile, the velocities in both wake regions change in the same trend and there is still a difference between them. In other words, the smaller gap ratio has an obvious effect on the vortex shedding in the gap but the effect is still weak. Therefore, the gap ratio change can not only have an influence on the center area between two cylinders but also make a great contribution to the flow regime of front and wake region.

For s/d = 1, velocity variation in the front area still exists as above described. Furthermore, the interference in the central area is significantly obvious. At first, the velocity is reduced more in the downstream wake region. It can be derived that vortex shedding has already occurred in the downstream wake region while it is suppressed in the central area. Nevertheless, the velocity is reduced more in central

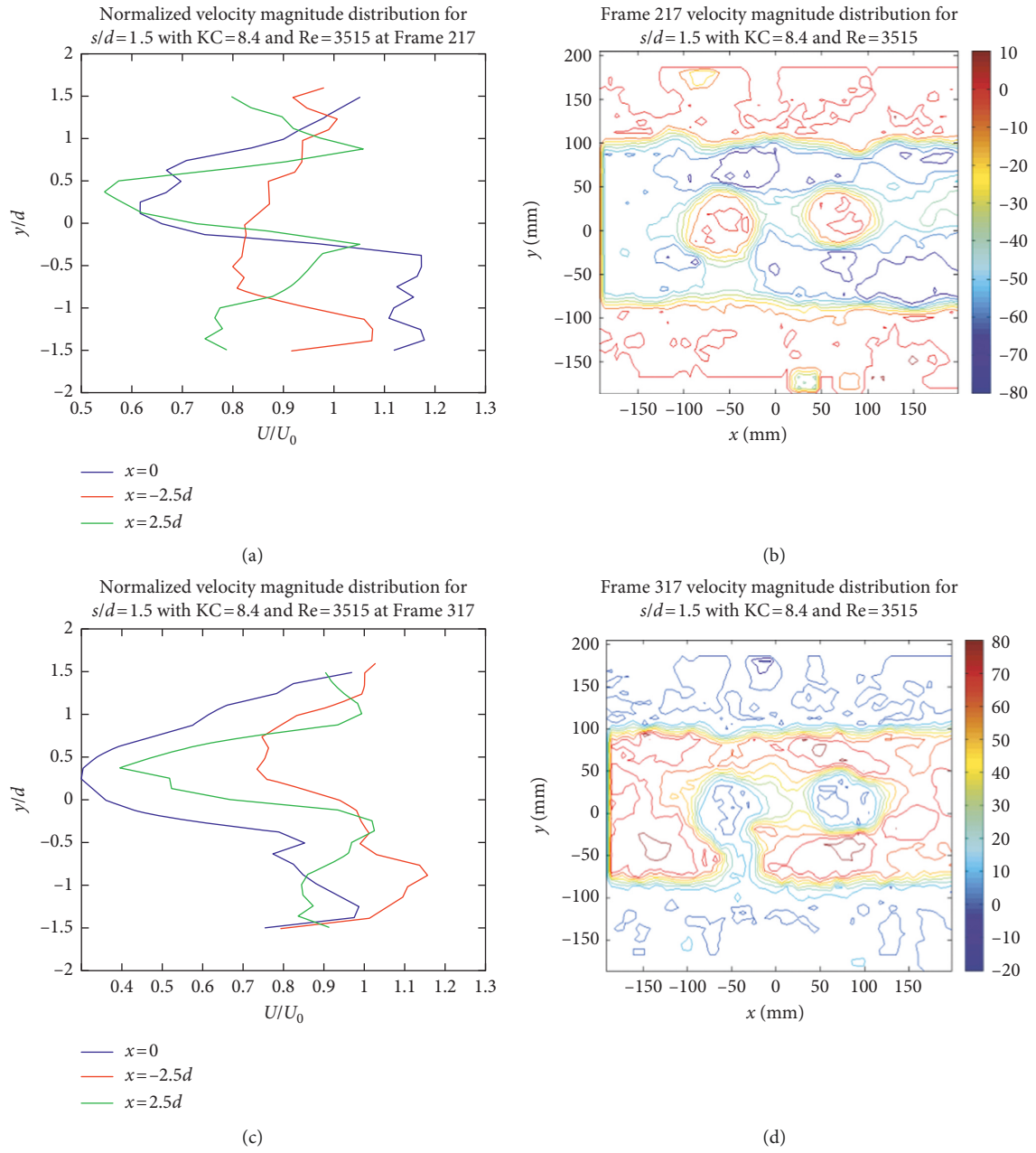

FIGURE 9: Normalized velocity and velocity contour when s/d = 1.5, Re = 3515.5, and KC = 8.4; (a) normalized velocity at Frame 217; (b) velocity magnitude contour at Frame 217; (c) normalized velocity at Frame 317; (d) velocity magnitude contour at Frame 317.

area in the next half period. It can be explained by that the cross gap flow due to the geometry of two cylinders pushes the fluid in the gap up or down, so the flow in gap just follows with the gap flow in vertical direction and horizontal velocity is reduced.

Five observation points are set to see the process of velocity with time, as shown in Figure 11. Figure 12 demonstrates the process of normalized velocity with different gap ratio s/d. According to the process of normalized velocity with time, the flow regime also shows a periodicity, and the period is still the half period of the whole flow motion. Point *D* and *E* have the same trend to some degree, so the effect of the gap ratio is relatively lower on the area of both sides. On the contrary, the velocity in the central area becomes completely different with a variation of gap ratio. As point B is located in the center of two cylinders, the velocity becomes more and more chaotic with two cylinders moving closer due to the interference of gap flow. Point A and C are located at the top and bottom area, and they have an opposite process compared with each other, which may be resulted from the vortex shedding formed at one side. However, with the gap smaller, the velocity on the top and bottom is no longer just periodically decreased or increased monotonously, which can be attributed to the gap cross flow formed. The interaction of gap flow and vortex shedding makes the motion more complex.

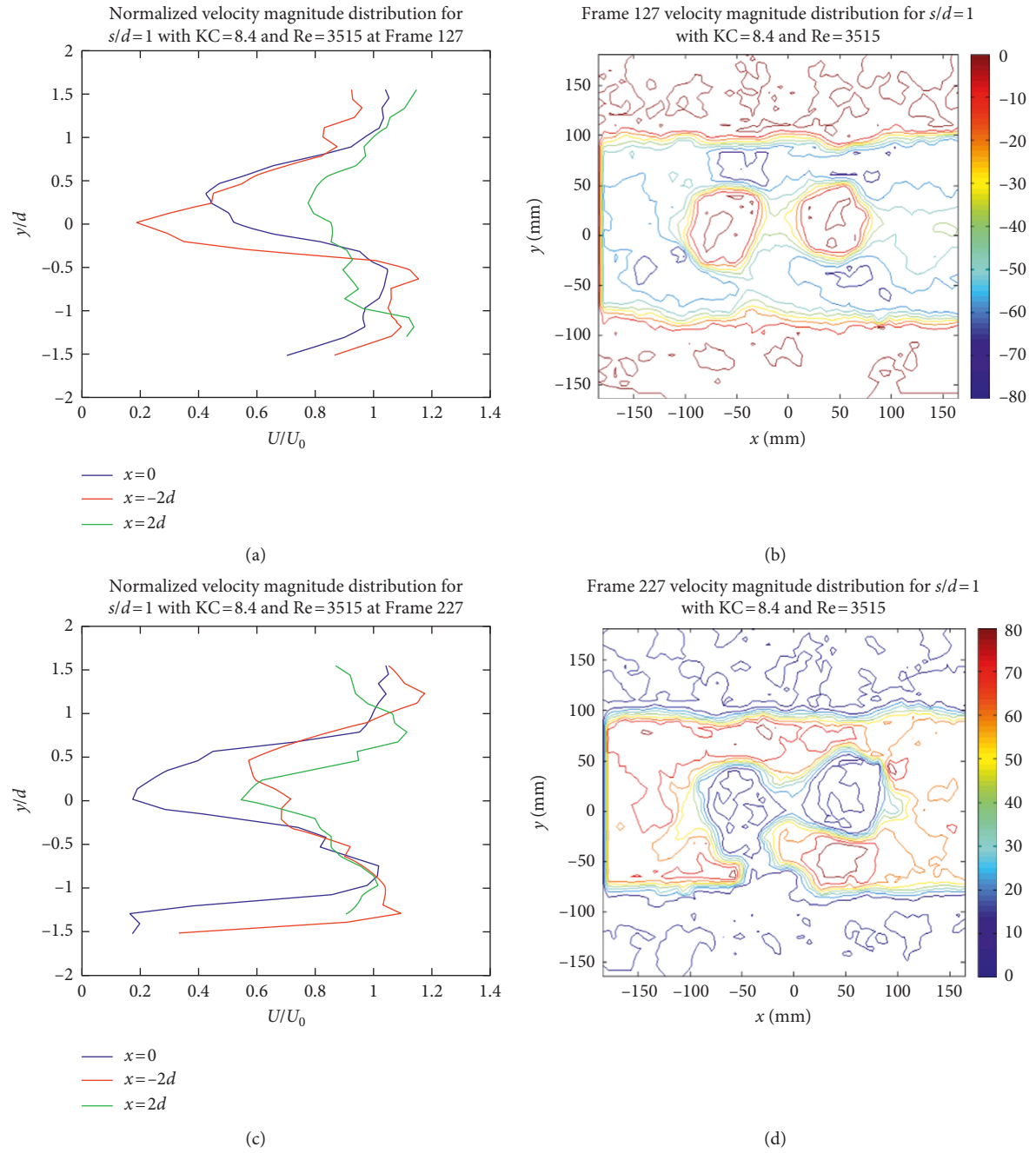

FIGURE 10: Normalized velocity and velocity contour when s/d = 1, Re = 3515.5, and KC = 8.4; (a) normalized velocity at Frame 127; (b) velocity magnitude contour at Frame 127; (c) normalized velocity at Frame 227; (d) velocity magnitude contour at Frame 227.

5. Conclusion

The particle image velocimetry (PIV) method is applied to measure the flow velocity field in different configurations to explore the effects of Re, KC, and gap ratio on flow separation around a cylinder array in oscillatory flows in this project.

The first configuration is oscillatory flow without cylinder in which the whole flow in the tube acts as oscillatory Poiseuille flow. Oscillatory flow without cylinder is uniform in the most spanwise area except for a considerably small boundary layer near top and bottom wall where the velocity is significantly small. So, the whole flow without cylinder can be regarded as a uniform flow, and it is also a cosine oscillatory flow which has a same period with the oscillatory motor motion.

The second configuration is two inline cylinders in oscillatory flow in which the effect of the gap ratio (s/d) is explored. Low KC cannot change the flow pattern around the cylinder, but smaller gap can decelerate the gap flow between cylinders. When KC = 8.4, vortex shedding will occur around each cylinder, and flow regime can be influenced significantly by the gap ratio.

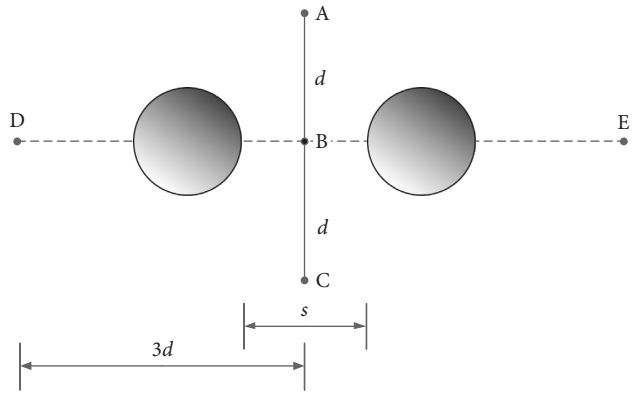

Figure 11: Five observation points.

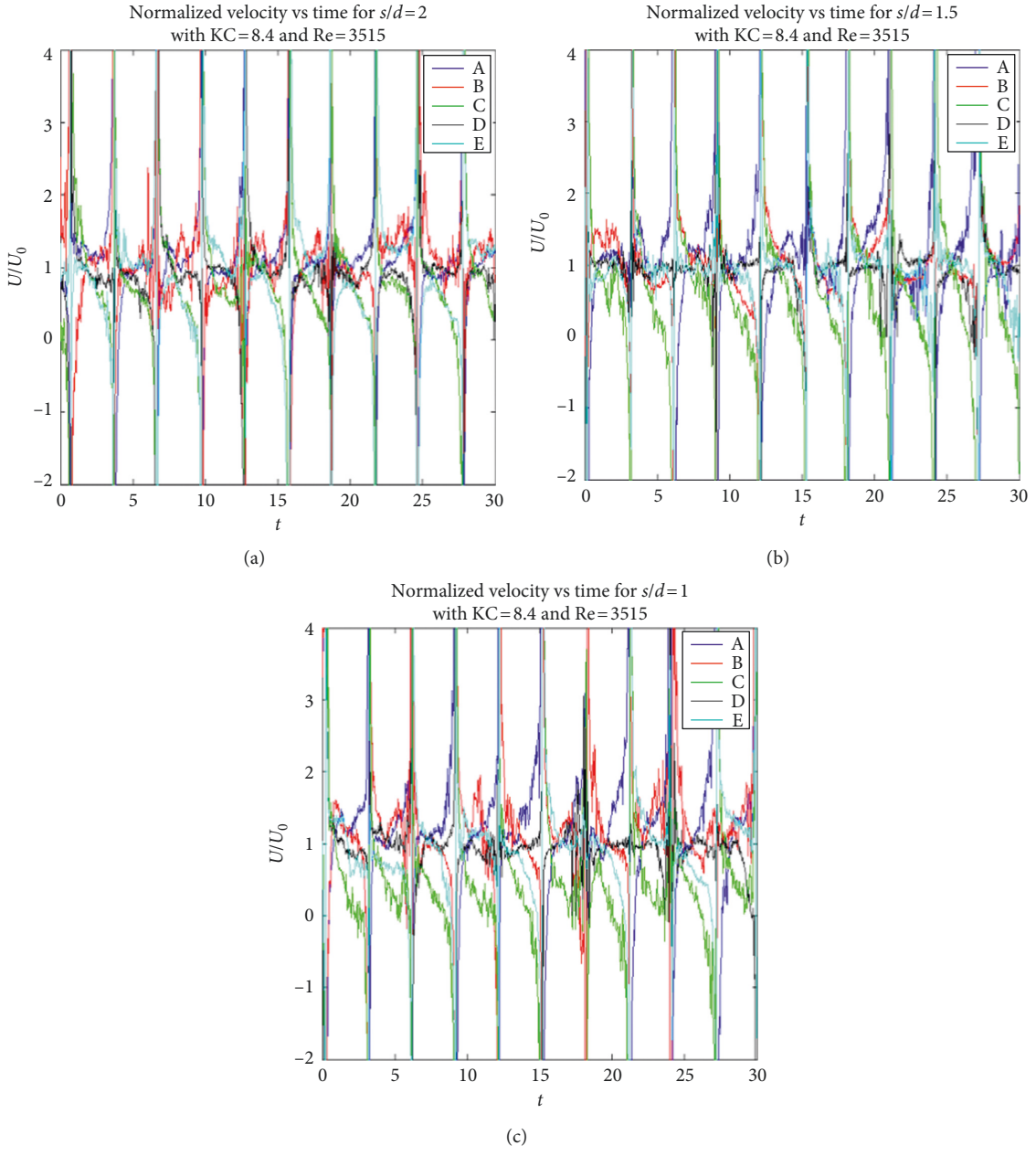

Figure 12: Normalized velocities with time for observation points, (a) s/d = 2, (b) s/d = 1.5, and (c) s/d = 1.

In fact, the flow separation pattern under such a configuration is mainly determined by the cylinder-to-cylinder gap ratio according to the above investigation. More specifically, the gap flow between two incline cylinders would shape the track of vortex shedding.

(a) At s/d = 2, gap flow follows the general cosine oscillatory Poiseuille flow, and gap flow velocity keeps pace with velocity in wake region. Consequently, unperturbed independent vortex shedding around each cylinder simultaneously is produced.

(b) At s/d = 1.5, the gap flow leads upstream vortex to attaching to the downstream cylinder so that upstream vortex interacts with downstream one and downstream vortex shedding goes further. Moreover, front velocity is significantly decreased due to the vortex shedding formed in last half period.

(c) As s/d decreases to 1, the gap flow transforms from horizontally to vertically. Velocity pattern at top of the gap is opposite to that at bottom of the gap, while velocity in wake region exhibits resemblances with that of s/d = 2. And the cross gap flow would orientate the vortex shedding and push vortices generated from upstream cylinder away from the downstream cylinder.

Generally speaking, this paper provides a new way to analyze flow separation around a cylinder array with PIV measurement. Observation of vortex shedding is transferred to observation of velocity field variation, and it can provide a quantitative analysis to some extent.

Data Availability

The data used to support the findings of this study are included within the article.

Conflicts of Interest

The authors declare that there are no conflicts of interest regarding the publication of this paper.

Acknowledgments

The authors would like to thank Prof. JunSheng Yang for excellent writing guidance. In addition, the authors also want to thank Prof. Francesco Franco for hard work and fair comments of this manuscript.

References

[1] B. K. Sumer and J. Fredsøe, *Hydrodynamics Around Cylindrical Structures*, World Scientific, Singapore, 2006.

[2] G. Schewe, "On the force fluctuations acting on a circular cylinder in crossflow from subcritical up to transcritical Reynolds numbers," *Journal of Fluid Mechanics*, vol. 133, no. 1, pp. 191–217, 1983.

[3] C. H. K. Williamson, "Oblique and parallel modes of vortex shedding in the wake of a circular cylinder at low Reynolds numbers," *Journal of Fluid Mechanics*, vol. 206, no. 1, pp. 579–627, 1989.

[4] C. P. Jackson, "A finite-element study of the onset of vortex shedding in flow past variously shaped bodies," *Journal of Fluid Mechanics*, vol. 182, no. 1, pp. 23–45, 1987.

[5] C. H. K. Williamson, "The existence of two stages in the transition to three-dimensionality of a cylinder wake," *Physics of Fluids*, vol. 31, no. 11, pp. 3165–3168, 1988.

[6] H. Zhang, U. Fey, B. R. Noack, M. König, and H. Eckelmann, "On the transition of the cylinder wake," *Physics of Fluids*, vol. 7, no. 4, pp. 779–794, 1995.

[7] E. Achenbach, "Distribution of local pressure and skin friction around a circular cylinder in cross-flow up to $Re = 5\times10^6$," *Journal of Fluid Mechanics*, vol. 34, no. 4, pp. 625–639, 1968.

[8] G. Ilidas and P. Anagnostopoulos, "Viscous oscillatory flow around a circular cylinder at low Keulegan-Carpenter numbers and frequency parameters," *International Journal for Numerical Methods in Fluids*, vol. 26, no. 4, pp. 403–442, 1998.

[9] X. W. Lin, P. W. Bearman, and J. M. R. Graham, "A numerical study of oscillatory flow about a circular cylinder for low values of beta parameter," *Journal of Fluids and Structures*, vol. 10, no. 5, pp. 501–526, 1996.

[10] M. J. Chern, P. R. Kana, Y. J. Lu, I. C. Cheng, and S. C. Chang, "A CFD study of the interaction of oscillatory flows with a pair of side-by-side cylinders," *Journal of Fluids and Structures*, vol. 26, no. 4, pp. 626–643, 2010.

[11] P. Anagnostopoulos and C. Dikarou, "Numerical simulation of viscous oscillatory flow past four cylinders in square arrangement," *Journal of Fluids and Structures*, vol. 27, no. 4, pp. 212–232, 2011.

[12] M. J. Chern, W. C. Hsu, and T. L. Horng, "Numerical prediction of hydrodynamic loading on circular cylinder array in oscillatory flow using direct-forcing immersed boundary method," *Journal of Applied Mathematics*, vol. 2012, Article ID 505916, 16 pages, 2012.

[13] C. M. Sewatkar, R. Patel, A. Sharma, and A. Agrawal, "Flow around six in-line square cylinders," *Journal of Fluid Mechanics*, vol. 710, pp. 195–233, 2012.

[14] S. R. Kumar, A. Sharma, and A. Agrawal, "Simulation of flow around a row of square cylinders," *Journal of Fluid Mechanics*, vol. 606, pp. 369–397, 2008.

[15] Moog Animatics, *SmartMotor User's Guide*, Moog Animatics, Mountain View, CA, USA, 2013.

[16] Dalziel Research Partners, *DigiFlow User Guide, version 3.4*, Dalziel Research Partners, Cambridge, UK, 2012.

[17] H. Honji, "Streaked flow around an oscillating circular cylinder," *Journal of Fluid Mechanics*, vol. 107, no. 1, pp. 509–520, 1981.

[18] C. H. K. Williamson, "Sinusoidal flow relative to circular cylinders," *Journal of Fluid Mechanics*, vol. 155, pp. 141–174, 1985.

[19] M. Raffel, C. E. Willert, S. T. Wereley, and J. Kompenhans, *Particle Image Velocimetry: A Practical Guide*, Springer, New York, NY, USA, 2007.

[20] Z. M. Cao, K. Nishino, S. Mizuno, and K. Torii, "Piv measurement of internal structure of diesel fuel spray," *Experiments in Fluids*, vol. 29, pp. S211–S219, 2000.

[21] D. Dennis, J. D. Nico, J. H. C. Herman, and W. Willem, "Characterization of spray-induced turbulence using fluorescence PIV," *Experiments in Fluids*, vol. 59, no. 7, p. 110, 2018.

[22] W. Kosiwczuk, A. Cessou, M. Trinité, and B. Lecordier, "Simultaneousvelocity field measurements in two-phase flows for turbulent mixingof sprays by means of two-phase piv," *Experiments in Fluids*, vol. 39, no. 5, pp. 895–908, 2005.

[23] J. Westerweel, G. E. Elsinga, and R. J. Adrian, "Particle image velocimetry for complex and turbulent flows," *Annual Review of Fluid Mechanics*, vol. 45, no. 1, pp. 409–436, 2013.